



Optimization of measurement of mitochondrial electron transport activity in postmortem human brain samples and measurement of susceptibility to rotenone and 4-hydroxynonenal inhibition

Gloria A. Benavides^a, Toni Mueller^a, Victor Darley-USmar^a, Jianhua Zhang^{a,b,*}

^a Department of Pathology, Mitochondrial Medicine Laboratory, Birmingham, AL, 35294, USA

^b Birmingham VA Medical Center, University of Alabama at Birmingham, Birmingham, AL, 35294, USA

ARTICLE INFO

Keywords:

Bioenergetics
Citrate synthase
Lactate dehydrogenase
Electron transport chain activities
Postmortem human brain tissues

ABSTRACT

Mitochondrial function is required to meet the energetic and metabolic requirements of the brain. Abnormalities in mitochondrial function, due to genetic or developmental factors, mitochondrial toxins, aging or insufficient mitochondrial quality control contribute to neurological and psychiatric diseases. Studying bioenergetics from postmortem human tissues has been challenging due to the diverse range of human genetics, health conditions, sex, age, and postmortem interval. Furthermore, fresh tissues that were in the past required for assessment of mitochondrial respiratory function were rarely available. Recent studies established protocols to use in bioenergetic analyses from frozen tissues using animal models and cell cultures. In this study we optimized these methods to determine the activities of mitochondrial electron transport in postmortem human brain. Further we demonstrate how these samples can be used to assess the susceptibility to the mitochondrial toxin rotenone and exposure to the reactive lipid species 4-hydroxynonenal. The establishment of such an approach will significantly impact translational studies of human diseases by allowing measurement of mitochondrial function in human tissue repositories.

1. Introduction

Mitochondria are important for cellular energy production, metabolite homeostasis, and cell signaling. Dysfunction of mitochondria, due to mitochondrial DNA mutations, deficiencies in electron transport chain activities, and deficits in glucose and lipid metabolism, are associated with aging and chronic pathologies including neurodegenerative diseases [1–11]. Mitochondrial toxins such as rotenone, paraquat, and MPTP have been shown to increase the risk for Parkinson's disease [12–16]. The lipid peroxidation product, 4-hydroxynonenal (HNE) has been shown to accumulate in both Parkinson's and Alzheimer's disease postmortem brains, and can severely impair mitochondrial function in experimental models [17–22]. Targeting mitochondrial bioenergetics has emerged as a therapeutic strategy for age-related neurodegenerative diseases [3,10,11,23–38]. We have previously reported a general method to investigate different facets of mitochondrial function and quality control analyses in cell culture based models [13]. It has proved technically challenging to translate these findings due to the restriction of human brain samples to post-mortem repositories.

Human postmortem brains have long provided important information about the conditions of diseases and aided the discoveries of amyloid deposit and tau tangles. Despite the brain imaging, measurement of CSF metabolites, and studies with isolated mitochondria, bioenergetics studies have been hampered by the lack of high throughput functional assays suitable for post-mortem samples [1,39–47]. These studies are also challenging because of limitations in materials, and the diverse range of human genetics, health conditions, sex, age, lifestyle, and tissue preservation. Using our previously published methods for the measurement of mitochondrial electron transport activities in frozen samples [48] we have modified and validated the method for human post-mortem brain samples. We have optimized the sample preparation methods to yield activities for mitochondrial complexes I-IV. Further, we demonstrate *ex vivo* the methods for determining dose response curves for the complex I inhibitor rotenone and the reactive lipid species 4-hydroxynonenal (4-HNE) in tissue homogenates prepared from individual brain samples. These data are a proof of principle for the application of these methodology to human brain repositories to provide key energetic data that has not previously been available.

* Corresponding author. Department of Pathology University of Alabama at Birmingham, BMRII-534, 901 19th Street S., Birmingham, AL, 35294-0017, USA.
E-mail address: jianhuazhang@uabmc.edu (J. Zhang).

<https://doi.org/10.1016/j.redox.2022.102241>

Received 23 December 2021; Received in revised form 12 January 2022; Accepted 14 January 2022

Available online 19 January 2022

2213-2317/© 2022 The Authors.

Published by Elsevier B.V. This is an open access article under the CC BY-NC-ND license

(<http://creativecommons.org/licenses/by-nc-nd/4.0/>).

Table 1

Human subjects.

Subject ID	Age	Sex	Race	PMI (hours)	Brain Hemisphere
A	84	F	W	7	Left
B	86	M	W	4	Right
C	74	F	W	3	Left

Abbreviations: Postmortem interval (PMI), male (M), female (F), white (W).

2. Method

2.1. Chemicals

4-HNE (32100) was purchased from Cayman. Antimycin-A (A8674), rotenone (R8875) succinic acid (S3674), β -Nicotinamide adenine dinucleotide, reduced disodium salt hydrate (NADH; N8129), Cytochrome *c* from equine heart (C2506), Alamethicin from *Trichoderma viride* (A4665), N,N,N',N'-Tetramethyl-p-phenylenediamine (TMPD; T7394), Ascorbate (A-7631) were obtained from Sigma. Tetramethylhydroquinone (T0822) was purchased from TCI America and sodium azide (S2271) from Fisher Chemical.

2.2. Human subjects and tissue acquisition

De-identified postmortem tissues were obtained from the Alabama Brain Collection in compliance with the University of Alabama at Birmingham Institutional Review Board protocol. Tissue samples consisted of gray matter from superior/middle temporal cortex from 3 individuals (Table 1). These samples were 1–2 cm² from approximately the same area of superior temporal gyrus (Brodmann Area 22). Following brain removal, assessments of neuropathology were conducted and individuals were excluded from the study if they had been diagnosed with any neurological or neurodegenerative disorder or if there was neuropathological evidence of neurodegenerative disease. Tissue chunks were then pulverized to a fine powder over liquid nitrogen and a small amount of the powder was subsequently homogenized and stored at –80 °C before being used in the assay. It is not possible to distinguish different cortical layers from these samples, as the powdered temporal cortex tissue as well as the homogenates prepared from the powdered cortex are a blend of cell types obtained from the same approximate brain region.

2.3. Human tissue processing and homogenization

Tissue fragments from human subjects were pulverized into a fine powder using a mortar and pestle over liquid nitrogen. Aliquots containing approximately 20 mg wet weight of brain tissue powder were mechanically homogenized in 10x volume of buffer containing 220 mM mannitol, 70 mM sucrose, 10 mM KH₂PO₄, 5 mM MgCl₂, 1 mM EGTA, 2 mM HEPES, pH7.2 (mitochondrial assay buffer (MAS)). Homogenates were incubated on ice for 10 min prior to centrifugation at 200×g, 500×g, or 1000×g for 10 min at 4 °C. Supernatants were collected and protein concentrations assessed by DC Lowry protein assay. Samples were either used immediately or stored at –80 °C.

2.4. Western blot analysis

Samples were prepared in 6x loading buffer (300 mM Tris-HCl, pH 6.8, 600 mM 1,4-dithiothreitol (DTT), 60% glycerol, 12% sodium dodecyl sulfate (SDS), 0.6% bromophenol blue), and 15 μ g protein loaded per lane in 12% Tris-Acrylamide gels. Proteins were electrophoresed and transferred onto nitrocellulose membranes, and probed for target proteins using primary antibodies against MT-CO1 (1:2000; ab14705, Abcam, Waltham, MA, USA) and VDAC1 (1:5000; ab14734, Abcam). Protein levels were quantified using Image Studio Lite v 5.2 (LICOR, Lincoln, NE, USA) and data analyzed using GraphPad Prism v. 8.4.3 software (GraphPad, San Diego, CA, USA) by two-way repeated measures ANOVA.

2.5. Bioenergetic assessment

As described previously [48], protein lysates at the indicated amounts in MAS buffer were loaded onto Seahorse XF96 microplates (Agilent, Santa Clara, CA) and centrifuged at 2000×g for 20 min at 4 °C. No pre-treatment of the plates was required. Then 160 μ l of MAS supplemented with Cytochrome *c* (10 μ M) and Alamethicin (10 μ g/ml) were then added to each well with a multichannel pipette pointed at 45° angle to avoid disrupting the homogenate adherence to the bottom of plate. Different substrates were added for complex I-IV assays: 1 mM NADH for complex I, 10 mM Succinate and 2 μ M Rotenone for complex II, 0.5 mM Duroquinol for complex III, 2 mM ascorbate and 0.5 mM TMPD (tetra methyl phenylene diamine) for complex IV. The last addition in the assays was 2 μ M Rotenone, 10 μ M AA or 20 mM Azide which were used to inhibit mitochondrial complexes.

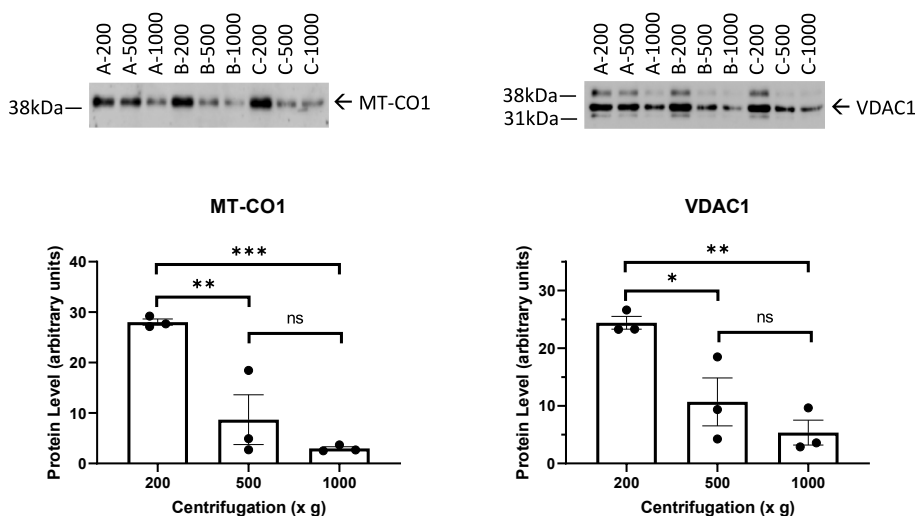


Fig. 1. Western blot analyses of Complex IV subunit 1, and VDAC effect of centrifugation rate. Protein levels of the mitochondrial markers MT-CO1 and VDAC1 in human brain homogenate samples from 3 human subjects processed at 200×g, 500×g, and 1000×g. Data are displayed as the mean \pm S.E.M. from 3 sample preparations from each subject at each centrifugation force. 2 way ANOVA indicates that there is a significant difference for centrifugation force. **p* < 0.05 compared to 200×g, and #*p* < 0.05 compared to 500×g, by post-hoc testing using the original FDR method of Benjamini and Hochberg.

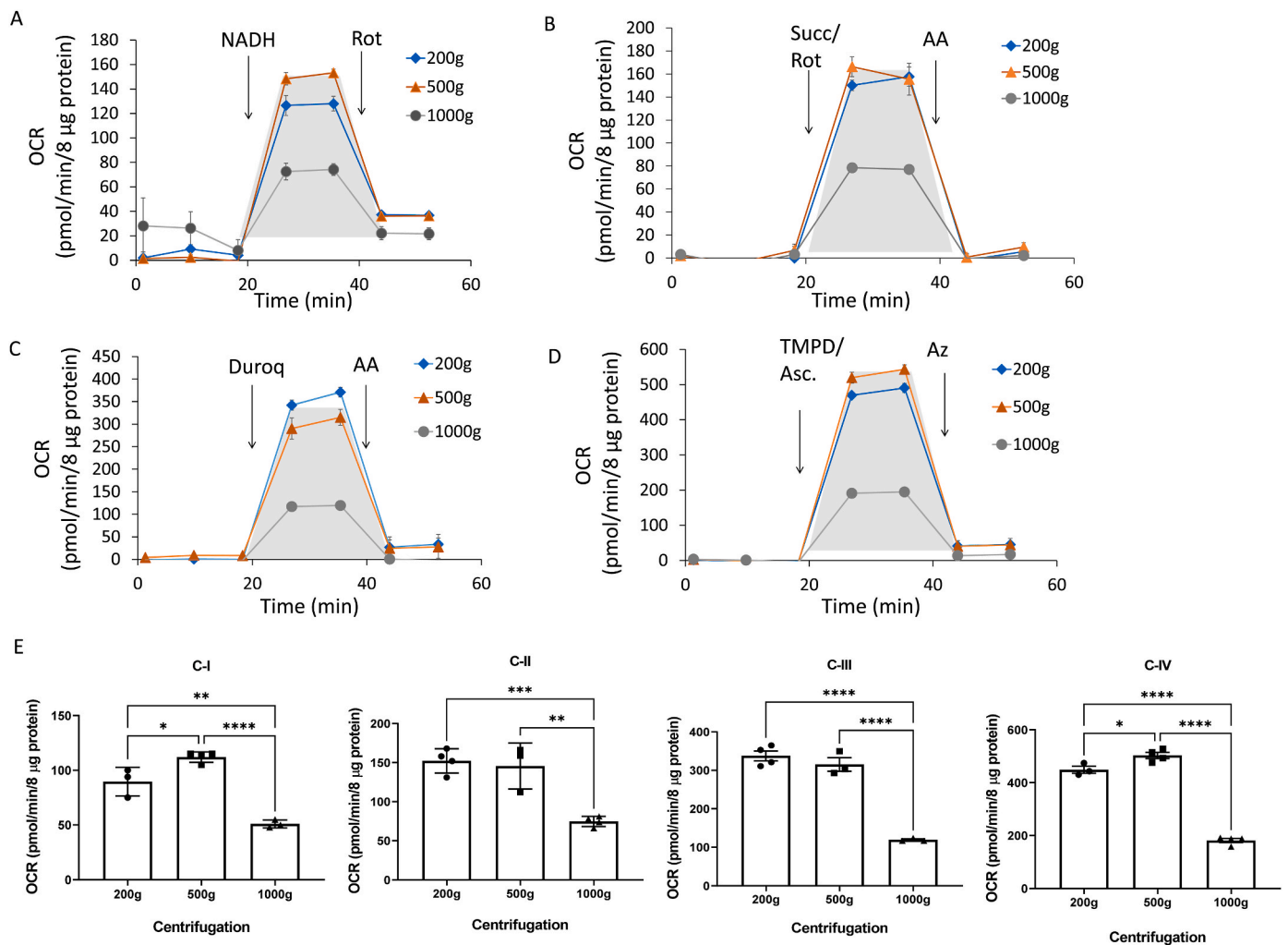


Fig. 2. Effect of centrifugation during sample preparation on complex I, II, III, and IV substrate linked respiration with postmortem brain samples. Postmortem sample A was used to test the effect of centrifugation during sample preparation on complex I, II, III, and IV substrate linked respiration (OCR) with postmortem brain samples. After sample preparation at the indicated centrifugation forces, 8 µg of protein was loaded per well ($n = 3-5$ technical replicates per sample preparation). Traces of complexes I (A), II (B), III (C), and IV (D) substrate linked respiration measured as described in Method. (E) Bar graphs comparing calculated complexes I-IV activities. Data are displayed as the mean \pm S.E.M.

2.6. Citrate synthase and LDHA activity assays

Citrate synthase and lactate dehydrogenase activities were measured using biochemical assays [48]. For citrate synthase activities, oxaloacetate, acetyl CoA, and DTNB were incubated with protein lysates. We then measured the product of DTNB-CoA at 412 nm, and calculated the activity as nmol/min/mg protein from the change of absorbance. For measurement of LDHA activities, NADH and Pyruvate were incubated with protein lysates. We then measured the disappearance of NADH absorption at 340 nm, and calculated the activity as nmols/min/mg protein from the change of absorbance.

2.7. Statistics for the XF analyses

Data are reported as mean \pm SEM. Comparisons among multiple groups were performed using a one-way analysis of variance (ANOVA), followed by post hoc Tukey's HSD test. A p -value of ≤ 0.05 was considered statistically significant. The IC₅₀ was calculated by Non-

linear regression log (inhibitor) vs. response with variable slope.

3. Results

3.1. Optimization of generating protein lysates for bioenergetics measurement from frozen human postmortem brain tissues

Recently we have established that mitochondrial electron transport chain activities can be measured using frozen protein lysates using the high throughput Seahorse XF bioanalyzer [48]. To apply this methodology to postmortem human brains we first investigated the optimal conditions for preparation of the protein lysates. We prepared cortical homogenates from 3 human subjects (A, B, and C) in lysis buffer compatible with Seahorse XF analyses, and removed debris using 3 different centrifugation forces: at 200 \times g, 500 \times g, or 1000 \times g. The supernatants were used for Western blot and Seahorse XF analyses.

Western blot analyses with 15 µg of lysates in 3 separate preparations of each of these centrifugation conditions were performed using

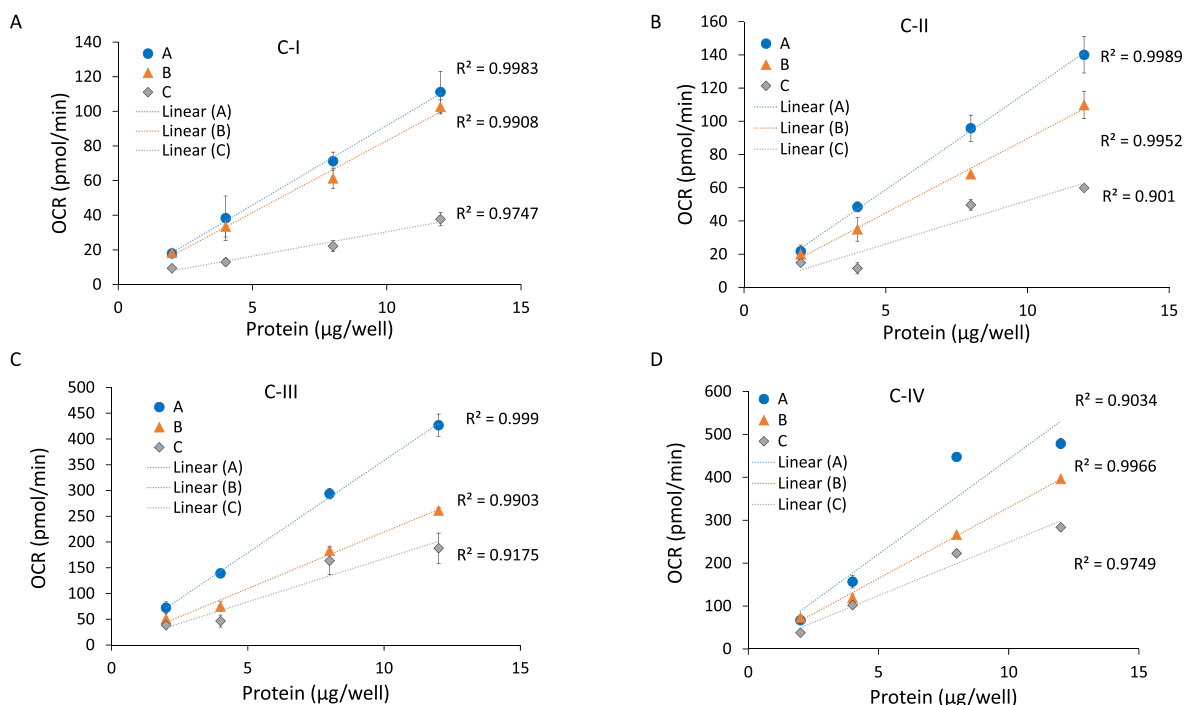


Fig. 3. Linear range of complex I, II, III, and IV substrate linked respiration with postmortem brain samples. Postmortem samples A, B and C were used to test the effect of amount of protein on complex I (A), II (B), III (C), and IV (D) substrate linked respiration (OCR) with postmortem brain samples. After sample preparation at 200×g, 2, 4, 8, and 12 µg of protein were loaded per well (n = 3–5 technical replicate wells per sample preparation). Complexes I (A), II (B), III (C), and IV (D) substrate linked respirations were measured as described in Method. Linear regression was used to determine the R² value. Data are displayed as the mean ± S.E.M.

antibodies against cytochrome c oxidase subunit I (MT-CO1) and voltage dependent anion channel 1 (VDAC1) as markers of mitochondrial content (Fig. 1). We found centrifugation at 200×g resulted in removal of cellular debris and greater retention of these mitochondrial marker proteins either 500×g or 1000×g.

Using one of the post-mortem brain samples (A), we compared the mitochondrial electron transport chain activities under these different centrifugation conditions. Shown in Fig. 2A–D are the typical profiles obtained using complex I–IV specific substrates and inhibitors. The shaded areas were used for calculation of the activities of each complex after subtracting the rate post addition of the specific inhibitor. We found that the 1000×g centrifugation resulted in attenuated mitochondrial respiration through complexes I, II, III and IV substrates compared to 200 and 500×g (Fig. 2A–D). Complex activities normalized to protein in the supernatant (the specific activity) are shown in Fig. 2E. Based on this data and that shown in Fig. 1 it is clear that 1000×g centrifugation results in a significant loss in mitochondrial proteins and their associated activities. In subsequent experiments the 200×g centrifugation condition was used for sample preparation.

3.2. The effect of lysate concentration on the mitochondrial electron transport chain activity

We next measured mitochondrial complexes I, II, III and IV substrate linked respiration in all 3 (A, B, and C) brain lysates with increasing amounts of protein per well to determine both linearity and the optimal concentration. As shown in Fig. 3, between 2 and 12 µg of lysates, complex I, II, III and IV substrate linked activities were linear with protein amount for all samples as expected (A, B, and C). Some differences between the different individuals in electron transport activities

were noted. For example, sample C had a lower complex I activity (Fig. 3A), and sample A had higher complex II, III and IV activities (Fig. 3B–D). From these data, a minimum amount of 8 µg protein is optimal for each complex resulting in an activity value with a low level of variation and efficient use of material. It is recommended that these calibration curves are performed with a typical sample before assaying a large cohort to ensure linearity and an optimal signal.

To have an independent measure of mitochondrial content and the efficiency of preparing the cell lysates, the activities of citrate synthase (CS), a mitochondrial matrix enzyme, and lactate dehydrogenase (LDH), a cytosolic enzyme were measured. Among the 3 independent brain samples, CS activities varied consistent with different amounts of mitochondria whereas LDH activities remained more consistent suggesting the homogenate preparation was similar between samples (Fig. 4A). The ratio of CS:LDH was also calculated and suggested an approximately 50% variation in mitochondrial content between samples. By normalizing the electron transport activities by CS activity this corrects for differences in mitochondrial number and can be used to determine whether the mitochondrial specific enzyme activity is lower in a given sample. When activities of complexes I, II, III and IV were normalized to CS activity in this way, the relationship between protein amount and activity become closer (Fig. 4B–E), compared to the values not corrected for CS activity (Fig. 3). However, lower complex I activity sample C and the higher complex III activity in sample A still evident, suggesting that there are intrinsic differences in these mitochondrial electron transport activities unrelated to mitochondrial mass (Fig. 4A, D). Comparing OCRs both with and without normalization to CS activities is necessary to determine whether a different mitochondrial activity is due to change of mitochondrial mass or change of specific activities of a given complex.

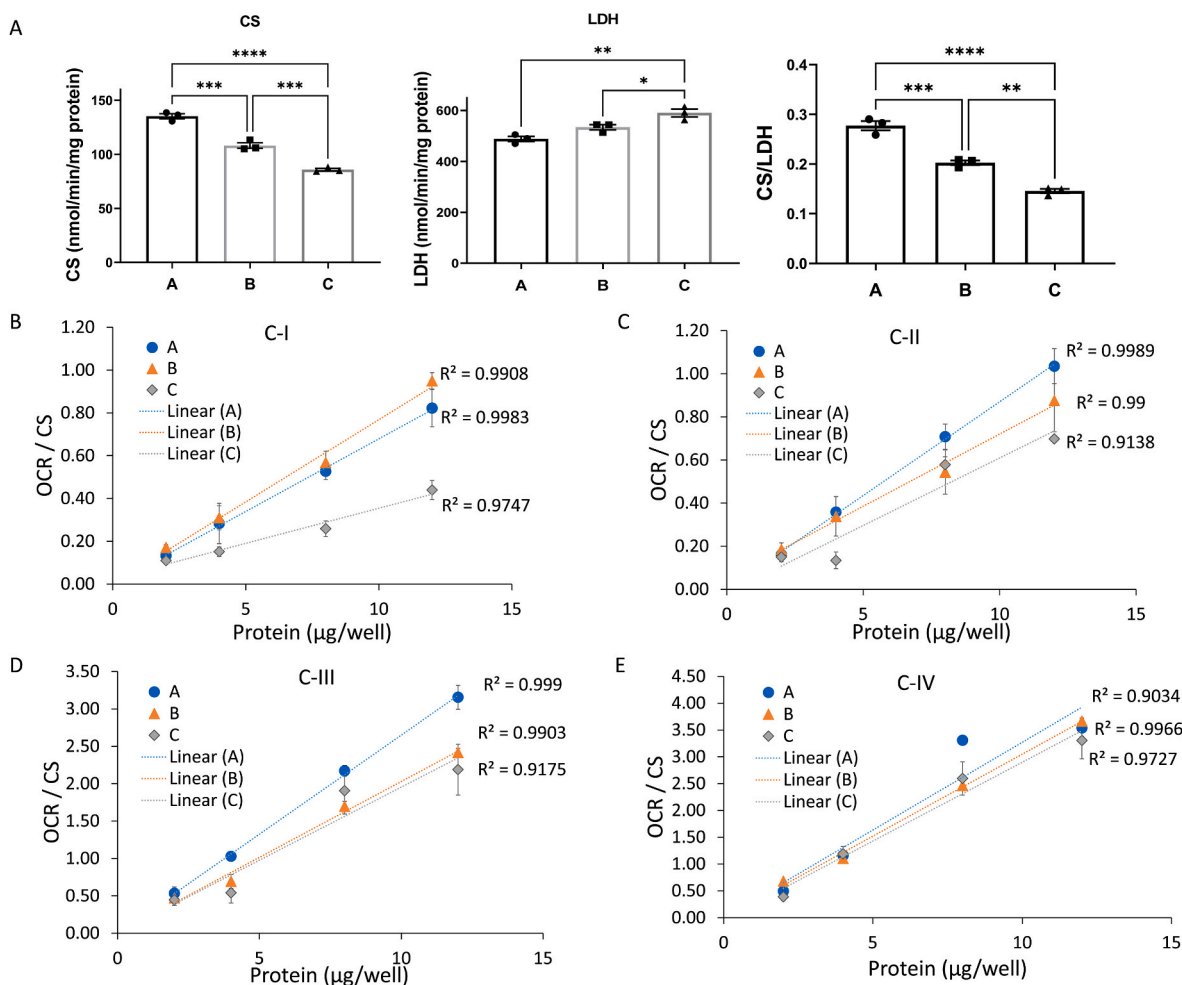


Fig. 4. Normalization of complex I, II, III, and IV substrate linked respiration to citrate synthase activities. (A) Bar graphs of citrate synthase (CS) activity, lactate dehydrogenase (LDH) activity, as well as the CS/LDH ratio. $n = 3$ technical replicates per sample. Then we normalized the complex I (B), II (C), III (D), and IV (E) substrate linked respiration (OCR) from Fig. 3 with respective citrate synthase activities. Linear regression was used to determine the R^2 value. Data are displayed as the mean \pm S.E.M.

3.3. Assessing susceptibility to neurotoxins in human brain lysates ex vivo

We then examined whether these protein lysates from frozen human postmortem brain tissues could be used to generate mitochondrial toxicity curves. We first incubated brain lysates with increasing concentrations of rotenone. As shown in Fig. 5A there is an inhibition of complex I substrate linked respiration in all 3 samples (A, B, and C). Complexes II, III, and IV linked respiration were unchanged by rotenone as expected and supporting the specificity of the assay and rotenone for complex I (Fig. 5B–D). After normalization to CS activity, the inhibition persisted while the differences between the three samples were decreased (Fig. 5E–H). The IC_{50} s for complex I inhibition were remarkably similar and consistent with literature values: A: 10.1 nM, B: 2.2 nM, and C: 2.2 nM (Fig. 5I) [16]. For example we have shown in primary neuron cultures, rotenone 10 nM immediately inhibited mitochondrial respiration and cell death occurs at 1 μ M after 2 h and 1 nM after 24 h [14].

To demonstrate the potential to assess susceptibility to toxins that are reactive to proteins we used the lipid peroxidation product 4-HNE. Protein-4-HNE adducts accumulate in Parkinson's and Alzheimer's

disease brains, and protein and organelle damage by 4-HNE has been shown to affect mitochondrial respiration in rodent primary neurons [17–22,49]. We next examined its effect on mitochondrial respiration in lysates from frozen human postmortem brain tissues. We found that there was a concentration dependent inhibition of complex I activity in the 10–500 μ M range (Fig. 6A). The inhibition of complexes II, III, and IV linked respiration were not as dramatic as complex I (Fig. 6B–E). As the case of rotenone, after normalization to CS activity, the effects persisted (Fig. 6E–H) with IC_{50} s for complex I inhibition of: A: 72.0 μ M, B: 55.0 μ M, and C: 52.0 μ M (Fig. 6I).

4. Discussion

In tissues and cell culture, the methods for assessing respiration with or without enrichment using mitochondrial preparations has been available for many years. However, only recently have high throughput methods been developed for frozen tissues [48,50] which have to be optimized for each specific tissue and complex activity. This new approach allows for the time needed for the transportation from a clinical setting to laboratories and measurement from tissues collected

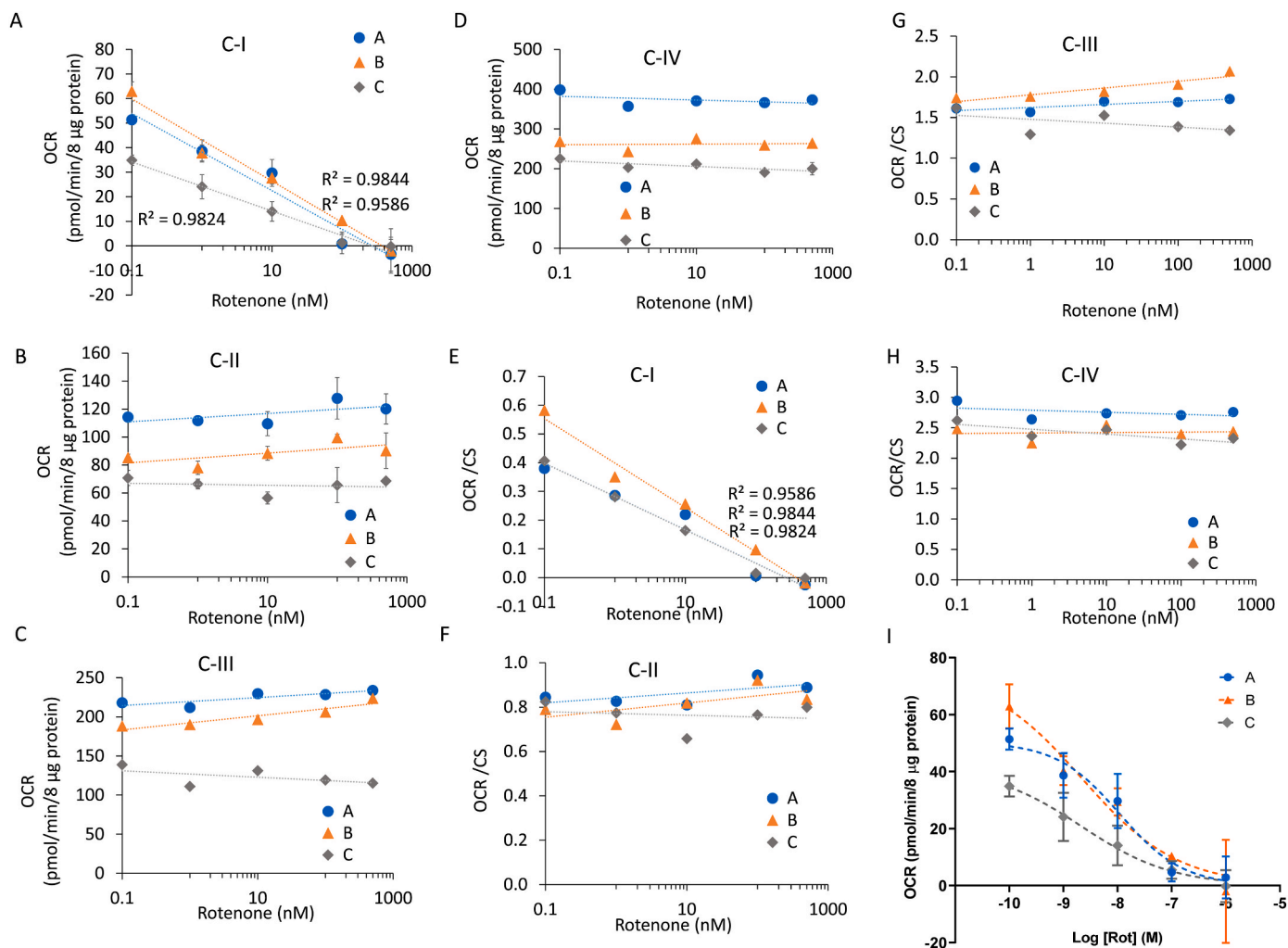


Fig. 5. Response of postmortem brain lysates to rotenone. Homogenates were pretreated with rotenone for 1 h at the indicated concentrations, followed by measurement of complex I (A,E), II (B,F), III (C,G), and IV (D,H) substrate linked respiration (OCR), with (E-H) and without (A-D) normalization to CS activities. (I) Linear regression was used to determine the R^2 value for complex I. Log regression fit was used to calculate IC50. Data are displayed as the mean \pm S.E.M.

over several years in biorepositories. In addition, throughput, isolation bias, consistency, and sensitivity is improved since it is no longer necessary to perform the multiple steps needed for mitochondrial purification.

In this study we demonstrate that the conditions of the centrifugation step needed for clearance of cellular debris are critical with a condition of $200\times g$ being optimal for human brain homogenates. Our study also demonstrates that the mitochondrial respiration is linearly proportional to the amount of homogenates with a dynamic range that can be used to detect changes of mitochondrial respiration that may arise due to aging or neurodegenerative diseases with as little as 8–12 μg protein. Mitochondrial electron transport activities can be normalized to protein in the homogenate which identifies a change in overall activity. Additional experiments using citrate synthase as a surrogate for mitochondrial number can then be used to determine whether the change activity can be ascribed to a change in mitochondrial number or loss of function in a specific protein complex. There are several caveats associated with using human postmortem tissues. These include variation in the regions or layers of the brain that are sampled that may have intrinsic differences in mitochondrial content and activity. In addition, post-mortem

intervals are rarely the same and should be assessed as an independent variable in larger study cohorts. Further, it is important to recognize that once screening with the bioenergetic assay has been performed, as described in these methods, they can be confirmed with spectrophotometric and other functional assays that offer a higher degree of specificity in terms of assignment of activity values to specific complexes but need a greater amount of starting material.

A variety of environmental or endogenously produced toxins are thought to contribute to human neurodegenerative diseases. An important hypothesis is that the impact of these toxins varies between individuals because of intrinsic difference in their susceptibility. The approach we describe here shows how this data can be generated using brain tissue homogenates. These approaches cannot take into account the impact of differential metabolism in response to the same exposure to a toxin but they could lead to more insights into intrinsic susceptibility at the site of action of the neurotoxin. As a proof of concept we used the environmental toxin rotenone and the endogenously generated lipid peroxidation product 4-HNE that has been detected in human brain [12–22]. The sensitivity to rotenone may be dependent on the initial complex I activity as rotenone specifically inhibits this respiratory

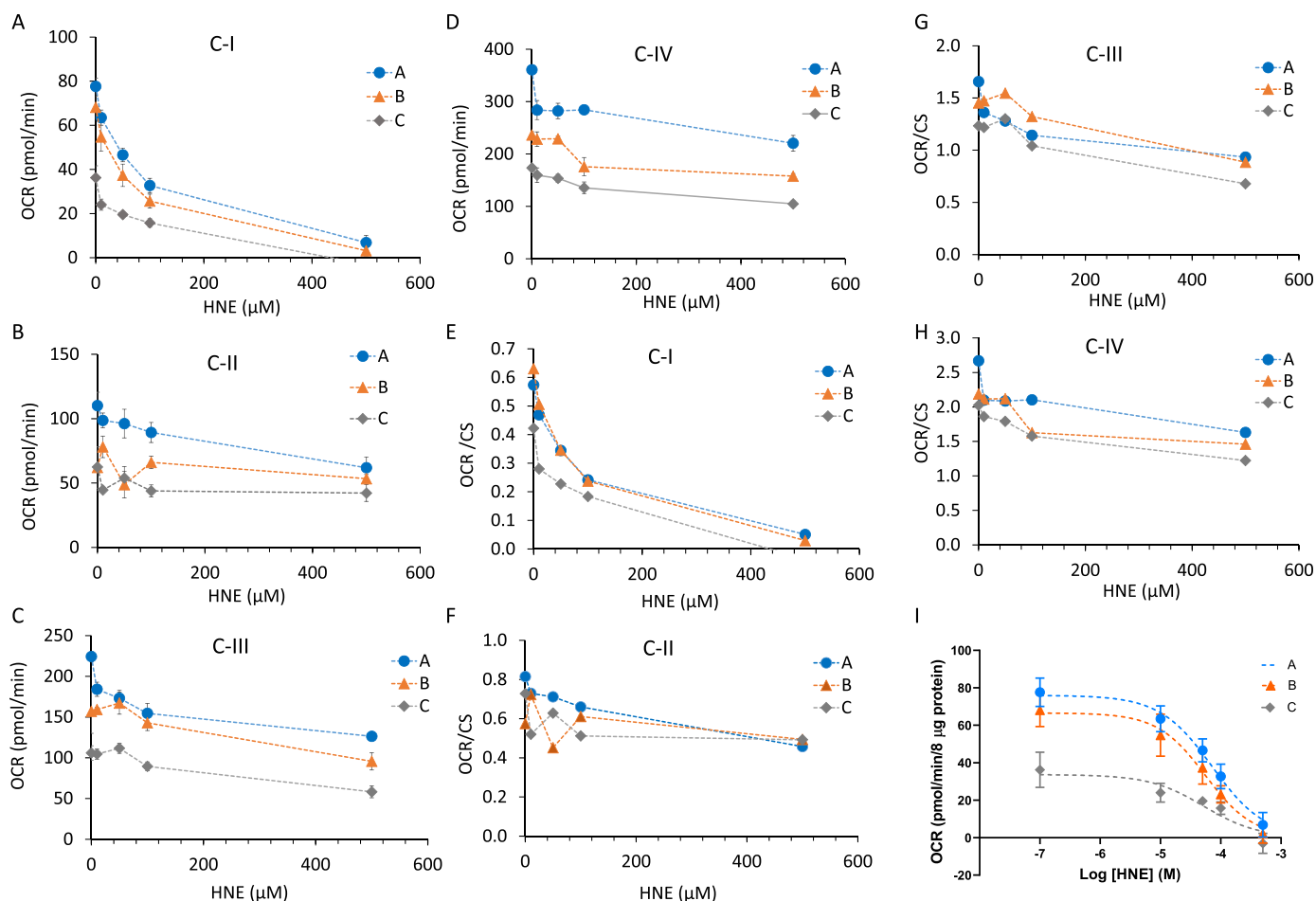


Fig. 6. Response of postmortem brain lysates to 4-HNE. Homogenates were pretreated with 4-HNE for 1 h at the indicated concentrations, followed by measurement of complex I (A,E), II (B,F), III (C,G), and IV (D,H) substrate linked respiration (OCR), with (E-H) and without (A-D) normalization to CS activities. Linear regression was used to determine the R^2 value for complex I. (I) Log regression was used to calculate IC_{50} . Data are displayed as the mean \pm S.E.M.

complex. Therefore, lower complex I activity due to genetic, environmental exposure or aging related complex I deficits, may result in higher sensitivity to rotenone. In a retrospective study this could then be correlated with clinical parameters related to the onset of neurodegenerative disease. In the case of 4-HNE it is endogenously produced through lipid peroxidation and has pleiotropic effects on mitochondrial function [49]. Sensitivity to 4-HNE is controlled by a number of factors including endogenous thiol status which could be revealed by the *ex-vivo* exposure assay illustrated here. These assays may then provide additional insights into susceptibility to oxidative stress that can be related to clinical parameters. In summary, we have shown a human brain homogenates obtained for a biorepository can be prepared from as little as 20 mg tissue and mitochondrial electron transport activities and susceptibility to toxins can be measured.

Funding

This work was supported in part by UAB Nathan Shock Center P30 AG050886 (VDU, JZ), R56AG060959 (JZ) and I01 BX-004251-01 (JZ).

Declaration of competing interest

The authors declare that they have no competing interests.

We thank the staff of the Alabama Brain Collection as well as the families and donors of the brain tissue used in this study.

References

- [1] S.N. Austad, T.W. Buford, C.S. Carter, D.L. Smith Jr., V. Darley-Usmar, J. Zhang, Targeting whole body metabolism and mitochondrial bioenergetics in the drug development for Alzheimer's disease, *Acta Pharm. Sin. B* (2021), <https://doi.org/10.1016/j.apsb.2021.06.0>.
- [2] J. Zhang, The promise of a golden era for exploring the frontiers of aging, metabolism and redox biology, *Front. Aging* 1 (2020) 4.
- [3] B.G. Hill, S. Shiva, S. Ballinger, J. Zhang, V.M. Darley-Usmar, Bioenergetics and translational metabolism: implications for genetics, physiology and precision medicine, *Biol. Chem.* 401 (1) (2019) 3–29.
- [4] R.H. Swerdlow, S. Koppel, I. Weidling, C. Hayley, Y. Ji, H.M. Wilkins, Mitochondria, cybrids, aging, and Alzheimer's disease, *Prog. Mol. Biol. Transl. Med.* 146 (2017) 259–302.
- [5] R.H. Swerdlow, J.M. Burns, S.M. Khan, The Alzheimer's disease mitochondrial cascade hypothesis: progress and perspectives, *Biochim. Biophys. Acta* 1842 (8) (2014) 1219–1231.
- [6] D.A. Butterfield, B. Halliwell, Oxidative stress, dysfunctional glucose metabolism and Alzheimer disease, *Nat. Rev. Neurosci.* 20 (3) (2019) 148–160.
- [7] B.W. Kunkle, B. Grenier-Boley, R. Sims, J.C. Bis, V. Damotte, A.C. Naj, et al., Genetic meta-analysis of diagnosed Alzheimer's disease identifies new risk loci and implicates Abeta, tau, immunity and lipid processing, *Nat. Genet.* 51 (3) (2019) 414–430.
- [8] G.S. Bloom, A. Norambuena, Alzheimer's disease as a metabolic disorder, *OCL* 25 (2018), D403.
- [9] L. Holper, D. Ben-Shachar, J.J. Mann, Multivariate meta-analyses of mitochondrial complex I and IV in major depressive disorder, bipolar disorder, schizophrenia, Alzheimer disease, and Parkinson disease, *Neuropsychopharmacology* 44 (5) (2019) 837–849.
- [10] R.H. Swerdlow, J.M. Burns, S.M. Khan, The Alzheimer's disease mitochondrial cascade hypothesis, *J. Alzheimer's Dis.* 20 (Suppl 2) (2010) S265–S279.
- [11] E.F. Fang, Y. Hou, K. Palikaras, B.A. Adriaanse, J.S. Kerr, B. Yang, et al., Mitophagy inhibits amyloid-beta and tau pathology and reverses cognitive deficits in models of Alzheimer's disease, *Nat. Neurosci.* 22 (3) (2019) 401–412.

- [12] J. Bove, C. Perier, Neurotoxin-based models of Parkinson's disease, *Neuroscience* 211 (2012) 51–76.
- [13] M. Redmann, G.A. Benavides, W.Y. Wani, T.F. Berryhill, X. Ouyang, M.S. Johnson, et al., Methods for assessing mitochondrial quality control mechanisms and cellular consequences in cell culture, *Redox Biol.* 17 (2018) 59–69.
- [14] S. Giordano, M. Dodson, S. Ravi, M. Redmann, X. Ouyang, V.M. Darley-Usmar, et al., Bioenergetic adaptation in response to autophagy regulators during rotenone exposure, *J. Neurochem.* 131 (5) (2014) 625–633.
- [15] S. Giordano, V. Darley-Usmar, J. Zhang, Autophagy as an essential cellular antioxidant pathway in neurodegenerative disease, *Redox Biol.* 2 (2014) 82–90.
- [16] S. Giordano, J. Lee, V.M. Darley-Usmar, J. Zhang, Distinct effects of rotenone, 1-methyl-4-phenylpyridinium and 6-hydroxydopamine on cellular bioenergetics and cell death, *PLoS One* 7 (9) (2012), e44610.
- [17] M. Dodson, Q. Liang, M.S. Johnson, M. Redmann, N. Fineberg, V.M. Darley-Usmar, et al., Inhibition of glycolysis attenuates 4-hydroxynonenal-dependent autophagy and exacerbates apoptosis in differentiated SH-SY5Y neuroblastoma cells, *Autophagy* 9 (12) (2013) 1996–2008.
- [18] L.M. Sayre, D.A. Zelasko, P.L. Harris, G. Perry, R.G. Salomon, M.A. Smith, 4-Hydroxynonenal-derived advanced lipid peroxidation end products are increased in Alzheimer's disease, *J. Neurochem.* 68 (5) (1997) 2092–2097.
- [19] M.A. Lovell, W.D. Ehmann, M.P. Mattson, W.R. Markesbery, Elevated 4-hydroxynonenal in ventricular fluid in Alzheimer's disease, *Neurobiol. Aging* 18 (5) (1997) 457–461.
- [20] A. Yoritaka, N. Hattori, K. Uchida, M. Tanaka, E.R. Stadtman, Y. Mizuno, Immunohistochemical detection of 4-hydroxynonenal protein adducts in Parkinson disease, *Proc. Natl. Acad. Sci. U. S. A.* 93 (7) (1996) 2696–2701.
- [21] B.G. Hill, B.P. Dranka, L. Zou, J.C. Chatham, V.M. Darley-Usmar, Importance of the bioenergetic reserve capacity in response to cardiomyocyte stress induced by 4-hydroxynonenal, *Biochem. J.* 424 (1) (2009) 99–107.
- [22] B.P. Dranka, G.A. Benavides, A.R. Diers, S. Giordano, B.R. Zelickson, C. Reily, et al., Assessing bioenergetic function in response to oxidative stress by metabolic profiling, *Free Radic. Biol. Med.* 51 (9) (2011) 1621–1635.
- [23] I.W. Weidling, R.H. Swerdlow, Mitochondria in Alzheimer's disease and their potential role in Alzheimer's proteostasis, *Exp. Neurol.* 330 (2020), 113321.
- [24] S.C. Cunnane, E. Trushina, C. Morland, A. Prigione, G. Casadesus, Z.B. Andrews, et al., Brain energy rescue: an emerging therapeutic concept for neurodegenerative disorders of ageing, *Nat. Rev. Drug Discov.* 19 (9) (2020) 609–633.
- [25] G. Rigotto, E. Basso, Mitochondrial dysfunctions: a thread sewing together Alzheimer's disease, diabetes, and obesity, *Oxid. Med. Cell. Longev.* 2019 (2019), 7210892.
- [26] M.P. Murphy, How mitochondria produce reactive oxygen species, *Biochem. J.* 417 (1) (2009) 1–13.
- [27] B. Kalyanaraman, Teaching the basics of redox biology to medical and graduate students: oxidants, antioxidants and disease mechanisms, *Redox Biol.* 1 (1) (2013) 244–257.
- [28] E.C.B. Johnson, E.B. Dammer, D.M. Duong, L. Ping, M. Zhou, L. Yin, et al., Large-scale proteomic analysis of Alzheimer's disease brain and cerebrospinal fluid reveals early changes in energy metabolism associated with microglia and astrocyte activation, *Nat. Med.* (26) (2020) 769–780.
- [29] N. Habib, C. McCabe, S. Medina, M. Varshavsky, D. Kitsberg, R. Dvir-Szternfeld, et al., Disease-associated astrocytes in Alzheimer's disease and aging, *Nat. Neurosci.* 23 (6) (2020) 701–706.
- [30] A. Webers, M.T. Heneka, P.A. Gleeson, The role of innate immune responses and neuroinflammation in amyloid accumulation and progression of Alzheimer's disease, *Immunol. Cell Biol.* 98 (1) (2020) 28–41.
- [31] A. Tarafdar, G. Pula, The role of NADPH oxidases and oxidative stress in neurodegenerative disorders, *Int. J. Mol. Sci.* 19 (12) (2018) 3824.
- [32] R. Afridi, J.H. Kim, M.H. Rahman, K. Suk, Metabolic regulation of glial phenotypes: implications in neuron-glia interactions and neurological disorders, *Front. Cell. Neurosci.* 14 (2020) 20.
- [33] A.M. Ibrahim, F.H. Pottou, E.S. Dahiya, F.A. Khan, J.B.S. Kumar, Neuron-glia interactions: molecular basis of Alzheimer's disease and applications of neuroproteomics, *Eur. J. Neurosci.* 52 (2) (2020) 2931–2943.
- [34] L.P. Bernier, E.M. York, B.A. MacVicar, Immunometabolism in the brain: how metabolism shapes microglial function, *Trends Neurosci.* 43 (11) (2020) 854–869.
- [35] C.M. Henstridge, B.T. Hyman, T.L. Spires-Jones, Beyond the neuron-cellular interactions early in Alzheimer disease pathogenesis, *Nat. Rev. Neurosci.* 20 (2) (2019) 94–108.
- [36] R.E. Gonzalez-Reyes, M.O. Nava-Mesa, K. Vargas-Sanchez, D. Ariza-Salamanca, L. Mora-Munoz, Involvement of astrocytes in Alzheimer's disease from a neuroinflammatory and oxidative stress perspective, *Front. Mol. Neurosci.* 10 (2020) 6844–6854.
- [37] L.A. Welikovitsh, S. Do Carmo, Z. Magloczky, J.C. Malcolm, J. Loke, W.L. Klein, et al., Early intraneuronal amyloid triggers neuron-derived inflammatory signaling in APP transgenic rats and human brain, *Proc. Natl. Acad. Sci. U. S. A.* 117 (12) (2020) 6844–6854.
- [38] S. Anwar, S. Rivest, Alzheimer's disease: microglia targets and their modulation to promote amyloid phagocytosis and mitigate neuroinflammation, *Expert Opin. Ther. Targets* 24 (4) (2020) 331–344.
- [39] N. Redjems-Bennani, C. Jeandel, E. Lefebvre, H. Blain, M. Vidailhet, J.L. Gueant, Abnormal substrate levels that depend upon mitochondrial function in cerebrospinal fluid from Alzheimer patients, *Gerontology* 44 (5) (1998) 300–304.
- [40] C. Liguori, A. Chiaravalloti, G. Sancesario, A. Stefani, G.M. Sancesario, N. B. Mercuri, et al., Cerebrospinal fluid lactate levels and brain [18F]FDG PET hypometabolism within the default mode network in Alzheimer's disease, *Eur. J. Nucl. Med. Mol. Imag.* 43 (11) (2016) 2040–2049.
- [41] L. Parnetti, A. Gaiti, M.C. Polidori, M. Brunetti, B. Palumbo, F. Chionne, et al., Increased cerebrospinal fluid pyruvate levels in Alzheimer's disease, *Neurosci. Lett.* 199 (3) (1995) 231–233.
- [42] Y. Chen, J. Wang, C. Cui, Y. Su, D. Jing, L. Wu, et al., Evaluating the association between brain atrophy, hypometabolism, and cognitive decline in Alzheimer's disease: a PET/MRI study, *Aging (N Y)* 13 (5) (2021) 7228–7246.
- [43] R. Marchitelli, M. Aiello, A. Cachia, M. Quarantelli, C. Cavaliere, A. Postiglione, et al., Simultaneous resting-state FDG-PET/fMRI in Alzheimer Disease: relationship between glucose metabolism and intrinsic activity, *Neuroimage* 176 (2018) 246–258.
- [44] R. La Joie, A. Perrotin, L. Barre, C. Hommet, F. Mezenge, M. Ibazizene, et al., Region-specific hierarchy between atrophy, hypometabolism, and beta-amyloid (Aβ) load in Alzheimer's disease dementia, *J. Neurosci.* 32 (46) (2012) 16265–16273.
- [45] R.L. Buckner, A.Z. Snyder, B.J. Shannon, G. LaRossa, R. Sachs, A.F. Fotenos, et al., Molecular, structural, and functional characterization of Alzheimer's disease: evidence for a relationship between default activity, amyloid, and memory, *J. Neurosci.* 25 (34) (2005) 7709–7717.
- [46] P. Edison, H.A. Archer, R. Hinz, A. Hammers, N. Pavese, Y.F. Tai, et al., Amyloid, hypometabolism, and cognition in Alzheimer disease: an [11C]PIB and [18F]FDG PET study, *Neurology* 68 (7) (2007) 501–508.
- [47] M.L. Schroeter, T. Stein, N. Maslowski, J. Neumann, Neural correlates of Alzheimer's disease and mild cognitive impairment: a systematic and quantitative meta-analysis involving 1351 patients, *Neuroimage* 47 (4) (2009) 1196–1206.
- [48] R. Acin-Perez, I.Y. Benador, A. Petcherski, M. Veliova, G.A. Benavides, S. Lagarrigue, et al., A novel approach to measure mitochondrial respiration in frozen biological samples, *EMBO J.* (2020), e104073.
- [49] M. Dodson, W.Y. Wani, M. Redmann, G.A. Benavides, M.S. Johnson, X. Ouyang, et al., Regulation of autophagy, mitochondrial dynamics, and cellular bioenergetics by 4-hydroxynonenal in primary neurons, *Autophagy* 13 (11) (2017) 1828–1840.
- [50] R. Acin-Perez, C. Beninca, B. Shabane, O.S. Shirihai, L. Stiles, Utilization of human samples for assessment of mitochondrial bioenergetics: gold standards, limitations, and future perspectives, *Life* 11 (9) (2021).